IJMOT

INTERNATIONAL JOURNAL OF MICROWAVE AND OPTICAL TECHNOLOGY

VOL.19, NO.5, SEPTEMBER 2024

Theoretical and Experimental Assessment of the Noise Levels, Arising at the Analog-to-Digital Conversion of the TV Broadcast Luminance Microwave Signals

Isa R. Mammadov[1], Islam J. Islamov[2*], Zafar A. Ismailov[3], Elvin I. Muradzade[1]

[1]Department of Electronics and Automation, Azerbaijan State Oil and Industry University, Azadliq ave. 20, AZ1010, Baku, Azerbaijan
isa.mammadov@asoiu.edu.az; muradzade.elvin36@gmail.com
[2]Department of Automation, Telecommunications and Energy, Baku Engineering University, Hasan Aliyev str., 120, AZ0101, Baku, Azerbaijan
isislamov@beu.edu.az
[3]Department of Radio Electronic and Aerospace Systems, Azerbaijan Technical University, H. Javid ave. 25, AZ1073, Baku, Azerbaijan
zafar.aleskeroqlu@mail.ru

Abstract **- The article presents a theoretical and experimental assessment of noise levels during the analog-to-digital conversion of TV broadcast microwave signals. Mathematical expressions are derived to calculate the mean quantization noise power for different brightness distribution models on TV images, considering both linear and nonlinear characteristics of the "light-to-signal" converter. For the first time, the dependence of the average quantization noise power on the compression coefficient is obtained for an inversely proportional distribution of brightness on the television image. This is particularly relevant when the input unipolar positive TV broadcast luminance signal is small, i.e., when the signal level is below the first quantization level. Additionally, analytical expressions are provided to calculate the level of restriction noise and the ratio of restriction noise power to quantizing noise power, particularly when the brightness distribution on TV images follows an exponentially decreasing model or an inversely proportional model with a logarithmic quantization scale. The impact of quantization and restriction noise on image quality was experimentally tested in an Additive White Gaussian Noise (AWGN) channel.**

Index Terms **- Microwave signals, Analog-to-Digital Conversion, Quantization Scale, Quantization Noise, Restriction Noise, Logarithmic Companding Method, TV Broadcast Luminance Signal Distribution.**

I. INTRODUCTION

The original analog television (TV) broadcast video signal, created at the television center, is converted into a standard digital television broadcast signal by using established algorithms. One of the first steps in this process is analog-to-digital conversion, which involves three operations: time sampling, level sampling (quantization), and encoding. Thus, the conversion of an analog signal into digital form can be divided into these three stages. For instance, in the MPEG-4 (Moving Picture Experts Group) algorithm, additional processes such as shape coding, motion compensation, texture coding, and binary and gradation coding of object information are also involved [1].

It is well-known that during analog-to-digital conversion, a limited amount of information is derived from an unlimited information, which inherently introduces sampling and quantization noise. The level of this noise, along with other parameters, depends on the quantizer's allowable range and the dynamic range of the quantized signal.

The quantization characteristics of each quantizer can generally be divided into three regions. The first region, known as the “empty channel”, corresponds to the small signal area. The signal level may be lower than the first quantization stage. This is the small signal range. Specific noises can occur at these low levels. In this case, two results are possible: depending on the state of the zero operating point of the quantizer characteristic, either no signal may appear at the output of the quantizer, or a discrete signal sequence (pulses corresponding to the first quantization level) may appear. This sequence of pulses can result from thermal noise, low-frequency network background, or harmonics of this background, even when the input signal to the quantizer is zero.

Due to the instability of the quantizer's operating point, if the quantized signal level is below the first quantization threshold, a signal corresponding to the first quantization level may appear at the quantizer's output. This “zero drift” relative to the input signal generates noise in the quiescent state, known as psophometric noise. Even by using modern stabilization methods, it is challenging to maintain complete stability at this point. Consequently, zero drift and fluctuations in sampling moments introduce additional noise during the analog-to-digital conversion process.

If the input of the quantizer with allowable quantization level M_y and quantization step Δ is supplied analog signal, which dynamic region is accordance to $-M_y\Delta/2 \div +M_y\Delta/2$, then the quantization of the signal is performed and this range is characterized by quantization noise [2].

Restriction (or overload) noise occurs when the quantized signal exceeds the maximum allowable value of the quantization level. The severity of this noise depends on how much the signal's dynamic range surpasses the quantizer's allowable range. This excess is quantified by a restriction factor (or restriction coefficient). The larger the restriction factor, the greater the restriction noise power introduced during quantization. This power also depends on other quantization parameters.

The levels of quantization noise and restriction noise can vary, making it essential to determine their power ratio. Both types of noise, along with other interfering factors, impact the quality of reproduced images. To assess the influence of these noises, we will conduct experimental research. However, it is difficult to directly quantify the contribution of these noises relative to other sources of interference.

II. PROBLEM FORMULATION

Digital TV broadcasting systems are generally characterized by high noise immunity. However, the presence of the aforementioned noises reduces this parameter to some extent. It is crucial to determine the degree of impacts each of these noises the system's noise immunity. Quantization noise, in particular, is associated with non-linear distortions. The levels of quantization error can be estimated in terms of the power of the quantization noises, the energy spectrum of these noises, or the voltage difference $u_{in} - U_n$, where u_{in} – voltage of the converted signal, U_n – n-th quantization evaluation level.

In [5], optimal controller synthesis is explored for a Linear-Quadratic-Gaussian quantized feedback system, where measurements must be quantized before being sent to the controller. The system is modeled with several quantizer options, each with an associated running cost. The objective is to jointly select the quantizers and controller to achieve an optimal balance between control performance and quantization cost. Under certain assumptions, this problem can be divided into two separate optimization problems: one for optimal controller synthesis and another for optimal quantizer selection.

In [6], single-bit Nyquist-rate quantization of randomly dithered sinusoids is studied for all-digital frequency synthesis. The study analytically derives the noise level caused by random dither and determines the output's

dynamic range. It also examines the trade-off between selective frequency notches and improvements in dynamic range.

In the work [7], the effect of quantization is compared for known deterministic synthesis methods. A method for reducing the computational cost of synthesis using an optimization approach is shown, and multi-criteria optimization is presented as a tool for achieving the desired beam shape and low sensitivity to quantization simultaneously.

In the work [8], results in the field of image recognition are presented. This work classifies objects in images using an efficient method for quantizing weights. It employs significantly fewer sample weights compared to the original weights.

The quantization step can be constant or variable. At the variable quantization step, the predicted values formed in the quantizer by various methods are used to control the thresholds [9-11].

A communication system where predicted values are based on previous values of the message signal is known as a predictive system. When using a variable quantization step, all quantizer thresholds are adjusted to the predicted quantization value. In Max and Diet-Panther quantizers, constant quantization estimation levels are used, with the quantization scale selected based on the signal's statistical properties [12, 13]. In the Max quantizer, for a non-uniform distribution of quantized voltage values, the quantization thresholds are chosen to minimize the power of the quantization noise. In the Diet-Panther quantizer at $\sum_{n=-N}^{N} w(u_n)\Delta u_n^3 = const$ this amount is kept to a minimum. In television, logarithmic quantization scales or uniform quantization with logarithmic companding are commonly used [14, 15]. In digital TV broadcasting, unipolar luminance and color signals are usually quantized separately. The level of quantization noise depends on the number of quantization levels, the quantization scale, and the distribution model of the quantized signal. However, the distribution of the TV broadcast luminance signal levels depends on the image structure and cannot be represented by a specific distribution model. Various models of this distribution and their prevalence are discussed in the literature [16].

It may be beneficial to separately identify the different types of quantization noise mentioned above. For the logarithmic companding method, it is necessary to calculate the average quantization noise power when the level of the quantized TV broadcast luminance signal is below the first quantization step for various distribution models. When the quantization step is small, the compression characteristic $y = f(u_{in})$ can be considered as follows:

$$\frac{\Delta y}{\Delta u_{in}} \approx \frac{dy}{du_{in}}, \qquad (1)$$

where $\Delta u_{in} = U_n - U_{n-1}, y(u_{in}) = dy/du_{in}$ – is the verticality of the compression characteristic.

Restriction noise occurs, when $K_U = U_{\max}/U_{Qu\max} > 1$, here K_U – is restriction coefficient, $U_{\max}$ – is the maximum value of the input signal, $U_{Qu\max}$ – is signal voltage corresponding to the maximum allowable value of the quantization threshold. Analog-to-digital conversion noise is combined with other types of noise. To experimentally evaluate such noises, it is essential to measure the amplitude-frequency characteristic, group delay, differential gain, and non-linear distortions in the TV broadcast signal, K – factor in 2*T* pulses. To evaluate traffic in a DVB system, the following parameters need to be measured: Bit Error Rate (BER), signal-to-noise ratio, and quadrature signal quality [17, 18]. Determining the overall level of noise generated by the quantizer is closely tied to its mode of operation. By dividing its operation into the three areas mentioned - quantization, restriction, and “empty channel” noise - it is possible to evaluate each type of noise separately. The literature has extensively discussed quantization noise levels.

However, restriction noise can be comparable to or even exceed the level of quantization noise. Therefore, a comparison of these two types of noise was conducted by calculating the ratio of their powers for different parameter values.

The purpose of this paper is to determine the level of quantization noises arising at the analog-to-digital conversion of TV broadcast luminance signals for various distribution models of brightness on TV images. It also aims to experimentally estimate the level of such noises at key measurement points in the system.

III. DETERMINATION OF DIFFERENT TYPES OF QUANTIZATION NOISES

Uniform quantization is easy to implement but often results in higher levels of quantization noise, making it less desirable. Non-uniform quantization can be performed directly with a non-uniform quantizer or indirectly through linear quantization after applying non-linear companding. Typically, the synthesis of a quantizer uses the criterion of minimizing the average root mean square quantization error [19].

To reduce quantization noise, several methods can be applied: increasing the number of quantization levels, choosing an appropriate step size, utilizing statistical characteristics of the processed signal, masking quantization noise, and optimizing the relationship between line frequency and sampling frequency.

Expressing brightness distribution in TV broadcast images using a specific model often does not fully represent reality. For example, one set of images may fit an inversely proportional model, another set may fit an exponentially decreasing model, and others may fit a normal distribution model. For these models, the level of quantization noise in TV broadcast luminance signals can be determined. As previously mentioned, various types of noise are introduced during the quantization process. Determining the level of these noises is crucial for assessing the signal-to-quantization noise ratio. First, let's calculate the quantization noise power for a small input value of the unipolar positive TV broadcast luminance signal. In this case, the quantization noise power can be determined using the following expression [20].

$$P_{Qu}(u_{in}) = \frac{1}{3N^2\left[y'(u_{in})\right]^2}, \qquad (2)$$

where N – is the number of evaluation levels of quantization, $y(u_{in})$ – is a compression characteristic.

When the logarithmic compression characteristic is applied, for the luminance signal of the TV images can be write [21].

$$y = \frac{U_{\max}\ln\left(1 + a\frac{u_{in}}{U_{\max}}\right)}{\ln(1+a)}, \qquad (3)$$

where a – compression coefficient at logarithmic companding of the signal (its value is determined experimentally), $U_{\max}$ – is the maximum value of the signal.

From the formula (3) is found:

$$y'(u_{in}) = \frac{a}{\left(1 + a\frac{u_{in}}{U_{\max}}\right)\ln(1+a)}. \qquad (4)$$

The slope of the tangent to the compression characteristic at the zero point is known as the compression coefficient [21]. The compression coefficient can be determined from the formula (4) for the logarithmic compression characteristic as follows:

$$K = y'(u_{in})\big|_{u_{in}=0} = \frac{a}{\ln(1+a)}. \qquad (5)$$

If replace (4) in the expression (2) we get:

$$P_{Qu}(u_{in}) = \frac{\ln^2(1+a)\left(1 + a\frac{u_{in}}{U_{\max}}\right)^2}{3N^2a^2}. \qquad (6)$$

The average value of the power of the quantization noise depends on the effective value of the signal and is calculated by the following expression:

$$\overline{P_{Qu}}(u_{in}) = \int_{-\infty}^{+\infty} P_{Qu}(u_{in})w(u_{in})du_{in}, \qquad (7)$$

where $w(u_{in})$ – is the one-dimensional

probability density of the signal voltage.

We have derived mathematical expressions for calculating the average power of quantization noise using various distribution models of brightness on TV images. Additionally, we have derived expressions (7) for both linear and nonlinear characteristics of the "light-to-signal" converter.

Dependence of the average value of quantization noise power on compression coefficient $\overline{P_{Qu}}(u_{in}) = f(K)$ for different values of α_0 and inverse proportional distribution of brightness on TV images is given (Figure 1).

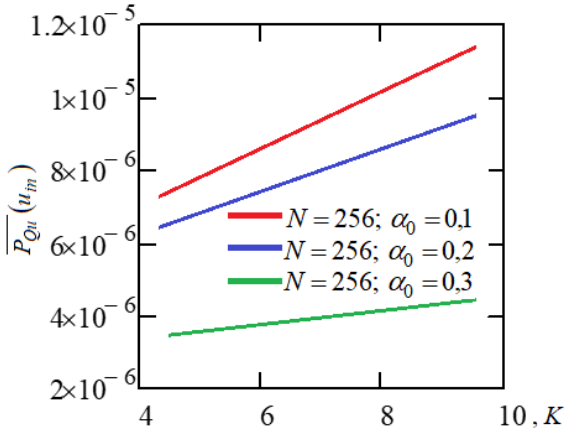

Fig. 1. Dependence of the average value of quantization noise power on the compression coefficient at inversely proportional distribution of brightness on the television images.

Here α_0 – is a constant, its values is determined experimentally. Values of α_0 depends on the characteristics of the TV images and the value $\alpha_0 = 0{,}2$ is the most repetitive. As can be seen from the Figure 1, for example, at *K*=8 when the value of α_0 increases from 0,1 to 0,3 the quantization noise power decreases by 2,5 times.

The graphs also indicate that as the compression coefficient decreases, the power of the quantization noise also decreases. However, a lower compression coefficient results in a reduced quantizer definition. Consequently, the impact of other types of noise increases, as the quantizer may mistake these other noises for quantized signals.

We are determined the value of $\overline{P_{Qu}}\left(\overline{u_{in}^2}\right)$ for different distribution of brightness on TV images. Quantization noise power with a linear light characteristic of the "light-to-signal" converter and an exponentially decreasing probability density of the TV broadcast luminance signal is define as [22-25]:

$$\overline{P}_{Qu}(u_{in}) = \frac{U_{\max}^2 \ln^2(1+a)}{3(2N+1)^2} \times$$
$$\times \left\{ 1 - 2a\frac{U_{mv}}{U_{\max}} \left[e^{-\frac{U_{\max}}{U_{mv}}} \left(\frac{U_{\max}}{U_{mv}} + 1 \right) - 1 \right] - a^2 \frac{U_{mv}^2}{U_{\max}^2} \times \right. \quad (8)$$
$$\left. \times \left[e^{-\frac{U_{\max}}{U_{mv}}} \left(\frac{U_{\max}^2}{U_{mv}^2} + 2\frac{U_{\max}}{U_{mv}} + 2 \right) - 2 \right] \right\},$$

where U_{mv} – is mean value of the input signal.

The obtained expression indicates that the quantization noise power can be calculated by the help of the maximum level of the luminance signal $U_{\max}$, the number of quantization levels *N* and experimentally obtained constant *a*. In this case, it is taken into account that the level of the quantized luminance signal is within the allowable quantization range of the quantizer and there is no restriction.

If we use the substitution $K_m = \frac{U_{mv}}{U_{\max}}$, we can simplify the expression (8):

$$\overline{P_{\text{Qu}}}(u_{in}) = \frac{U_{\max}^2 \ln^2(1+a)}{3(2N+1)^2} \times$$
$$\times \left\{ 1 - 2aK_m \left[e^{-\frac{1}{K_m}} \left(\frac{1}{K_m} + 1 \right) - 1 \right] - a^2 K_m^2 \times \right. \quad (9)$$
$$\left. \times \left[e^{-\frac{1}{K_m}} \left(\frac{1}{K_m^2} + 2\frac{1}{K_m} + 2 \right) - 2 \right] \right\}.$$

Similarly, we have derived an expression for calculating the quantization noise power for linear characteristics of the "light-to-signal" converters and an inversely proportional

distribution of brightness on TV broadcast images:

$$\overline{P}_{Qu}(u_{in}) = \frac{U_{\max}^2 \ln^2(1+a)}{3(2N+1)^2} \times$$
$$\times \left\{ 1 + 2a \left(\frac{1}{\ln \frac{\alpha_0 + 1}{\alpha_0}} - \alpha_0 \right) + a^2 \left[\frac{(1-\alpha_0)^2}{2 \ln \frac{\alpha_0 + 1}{\alpha_0}} + \alpha_0^2 \right] \right\}. \quad (10)$$

When the level of the TV broadcast luminance signal exceeds the maximum allowable quantization level, additional noise – restriction noise is generated. For a unipolar signal, the restriction noise power is determined by the known formula:

$$\overline{P}_{\mathrm{Re}}(u_{in}) = \frac{U_{\max}^2}{U_{Qu\max}^2} \int_{U_{Qu\max}}^{U_{\max}} (u_{in} - U_{Qu\max})^2 w(u_{in}) du_{in}, \quad (11)$$

where $w(u_{in})$ – input signal amplitude probability density, $U_{Qu\max}$ – is the maximum allowable quantization level of the quantizer.

Suppose the brightness distribution in TV images is exponentially decreasing. In this case, we have derived the following expression to calculate the restriction noise power:

$$\overline{P_{\mathrm{Re}}}(u_{in}) = -e^{-\frac{U_{\max}}{U_{mv}}} \times$$
$$\times \left(U_{\max}^2 + 2U_{\max}U_{mv} + 2U_{mv}^2 - 2U_{\max}^2 / K_U - \right. \quad (12)$$
$$\left. - 2U_{\max}U_{mv} / K_U + U_{\max}^2 / K_U^2 \right) +$$
$$+ 2U_{mv}^2 e^{-\frac{U_{\max}}{K_U U_{mv}}}.$$

When the distribution of the TV broadcast luminance signal levels is inversely proportional under the same conditions and a logarithmic quantization scale is applied, we have derived the following expression to calculate the level of these noises:

$$\overline{P}_{\mathrm{Re}}(u_{in}) = \frac{U_{\max}^2}{K_U^2 \ln \frac{\alpha_0 + 1}{\alpha_0}} \times \quad (13)$$
$$\times \left[\frac{K_U^2 - 1}{2} - (2 + \alpha_0 K_U)(K_U - 1) + (1 + \alpha_0 K_U)^2 \ln \frac{1 + \alpha_0}{1/K_U + \alpha_0} \right].$$

Therefore, the restriction noise power depends on the distribution model of the input signal, the quantization scale, the restriction coefficient, and the maximum allowable quantization level of the quantizer. It is important to note that restriction noise arises only when $K_U > 1$.

From the obtained expressions (12) and (13), it follows that the power of restriction (overload) noise is intricately dependent on the level of the restriction coefficient, even with a relatively simple distribution of the quantized signal values.

IV. POWER RATIO OF QUANTIZATION NOISE AND RESTRICTION NOISE FOR DIFFERENT TV BROADCAST LUMINANCE SIGNAL DISTRIBUTIONS

From the obtained expressions, it follows that if the dynamic range of the quantized signal is not appropriately chosen, restriction noises are added to the quantization noises. The levels of these noises depend on both the distribution model of the signal and the restriction coefficient. This leads to a decrease in the noise immunity of the system and an increase in signal distortion due to the limitation of the dynamic range of the signal. To understand which type of noise has the largest impact, we need to determine the ratio of these noise powers. It can be seen from the obtained expressions that this ratio is depends on the number of quantization level N, on the restriction coefficient K_U, on the value of constant quantities a and α_0, on the distribution model of the input signal, and on the quantization scale.

However, the obtained expressions do not provide a clear assessment of the levels of quantization and restriction noises. Therefore, it is necessary to represent the ratio of these noise powers in graphs or tables for different distributions of the quantized signal and applied quantization scales. Specifically, when the distribution model of the TV broadcast luminance signal is inversely proportional and a logarithmic quantization scale is applied, for α_0=0,2 and a=30 we calculate values $\overline{P}_{Qu}(u_{in})$, $\overline{P}_{\mathrm{Re}}(u_{in})$ and the ratio $\overline{\chi}(u_{in})$ of the restriction noise power to the quantization noise power (Table 1).

Table l: Quantization noise power and restriction noise power for different number of quantization levels and various values of the restriction coefficient

	$\overline{P}_{\mathrm{Re}}(u_{in})$	$\overline{P}_{Qu}(u_{in})$	$\overline{\chi}(u_{in})$
K_U=1,4; N=256	$7\cdot10^{-4}U_{\max}^2$	$33\cdot10^{-4}U_{\max}^2$	0,21
K_U=1,5; N=256	$77\cdot10^{-4}U_{\max}^2$	$33\cdot10^{-4}U_{\max}^2$	2,33
K_U=1,4; N=1024	$7\cdot10^{-4}U_{\max}^2$	$2{,}05\cdot10^{-4}U_{\max}^2$	3,41
K_U=1,5; N=1024	$77\cdot10^{-4}U_{\max}^2$	$2{,}05\cdot10^{-4}U_{\max}^2$	37,56

The Table 1 shows that an increase in the restriction coefficient from 1,4 to 1,5 leads to the 11-time increase in the power of the restriction noise. Also, when length of the code word in the binary system n (N=2^n) increased from 8 to 10, the power of the quantization noise decreases by 16 times. When the length of the code word, for the same restriction coefficient increase from 8 to 10 the ratio of the quantization noise power to the restriction noise power decreases by 16...17 times.

V. EXPERIMENTAL VERIFICATION OF THE EFFECT OF QUANTIZATION NOISES AND RESTRICTION NOISES ON IMAGE QUALITY

Evaluating the quality criteria of the DVB-T system is crucial. To assess the quality of the DVB system, two types of measurements are conducted: (a) parameters of the traffic stream and (b) quality parameters of channel equipment. The first type of measurements includes parameters such as Bit Error Ratio (BER), Signal-to-Noise Ratio (SNR), and the quality of quadrature signals [26-30]. The system uses a quality threshold criterion [31-34]. The Total Offset on Video (TOV) metric indicates the presence of numerous errors in the images. The Quasi-Error-Free (QEF) reception criterion is applied, where the BER at the output of the RS (Reed-Solomon) decoder is less than BER =10^{-11}. At the output of the Viterbi decoder (at the input of the RS decoder) errors should not be worse than BER=$2\cdot10^{-4}$. For measurement, we use a diagram that highlights the characteristic points important for assessment (see Figure 2). An analyzer was employed for the measurements. Signal power was measured at the input of the high-frequency converter and assessed within the nominal frequency band. Noise levels were measured by using the analyzer.

The experimentally studied channel—the Baku-Alat radio relay line - can be classified as an open track channel with Additive White Gaussian Noise (AWGN) [35, 36]. The “Iposolinc” transmitter-receiver station of NEC company was used as the relay station. The parameters of the digital TV broadcasting system were selected using an iterative method.

During the experiment, key parameters such as the guide interval (GI), bit rate, and Forward Error Correction (FEC) were selected. The measurement scheme for TV signal parameters is shown in Figure 3. For this type of channel, permissible signal-to-noise ratio values are known and depend on factors such as channel coding, phase noise, quantization noise, and intermodulation products. Consequently, the effect of quantization noise can only be assessed indirectly.

In order to assess the quality of the system, it is more convenient to use the ratio of bit energy to the spectral density of noise:

$$\frac{E_b}{N_0}=\frac{P_s}{P_N}-10\lg\left(\frac{R_b}{\Delta f}\right), \qquad (14)$$

where E_b – is bit energy, N_0 – is noise intensity, P_s – is signal carrier power, $P_N=\frac{N_0}{2T_b}$ – is power of noise, R_b – is transmission rate, Δf – system bandwidth, T_b – is the duration of the bit.

$\frac{E_b}{N_0}$ and $\frac{P_0}{P_N}$ – ratios were measured. The signal power was measured at the input of the high frequency converter and assessed within the nominal frequency band. Noise levels were measured using an analyzer by turning off the

subcarriers. Table 2 shows the selected values and the obtained results.

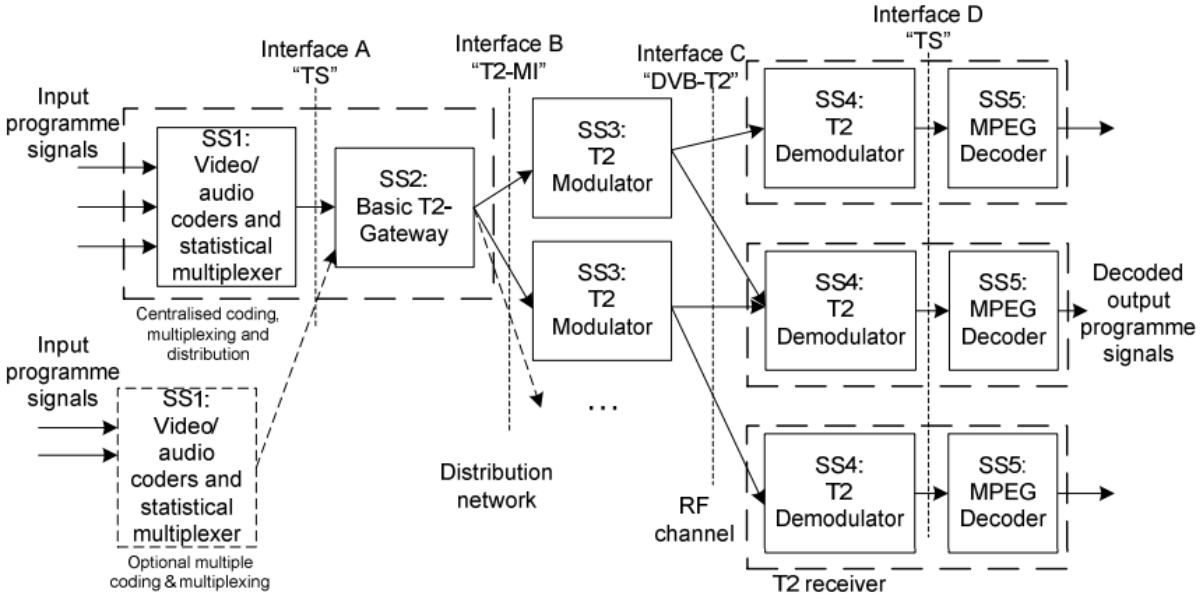

Fig. 2. Diagram for measuring parameters showing characteristic points.

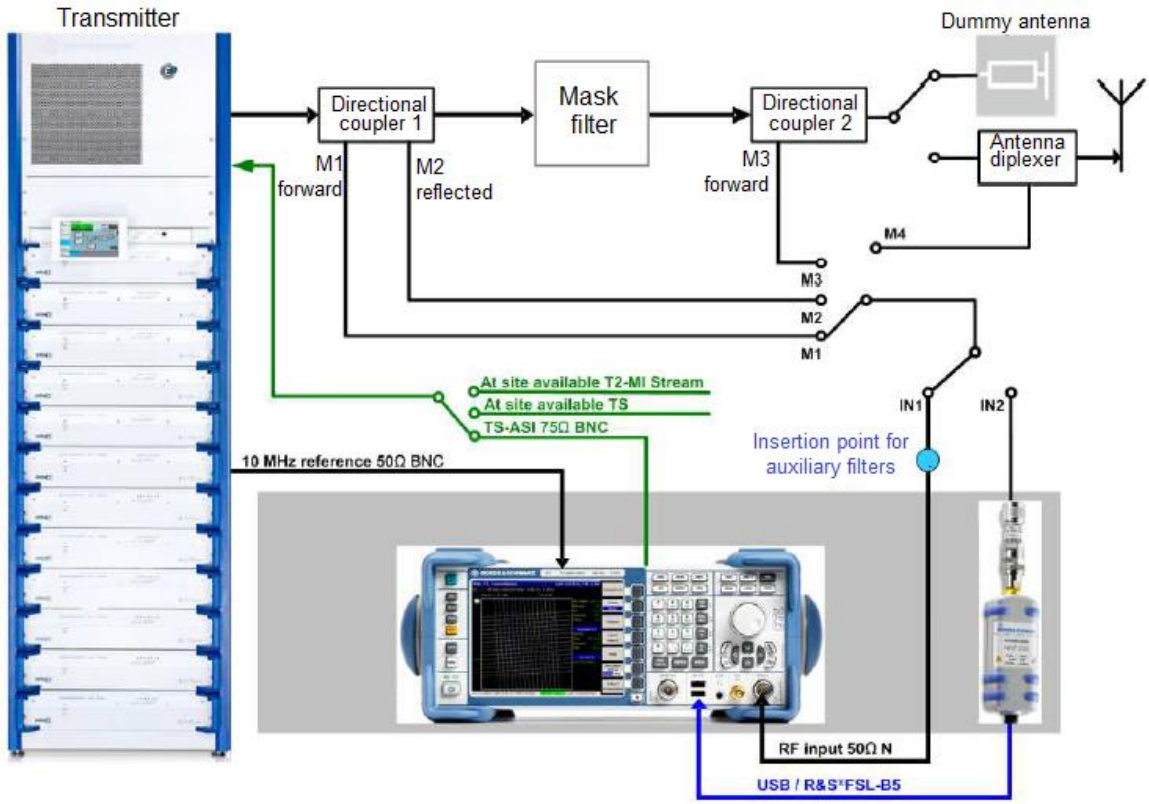

Fig. 3. Scheme for measuring TV signal parameters.

The Table 2 shows that the required value of QEF should be 1,3 *dB* higher than the corresponding value of TOV. During the experiments, it was observed that the difference was slightly greater.

Table 2: Signal-to-interference ratio on AWGN channel in DVB-T system

References	E_b / N_0 ratio values, *dB*		P_s / P_N ratio values, *dB*	
	Required	Experimental	Required	Experimental
[5]	10,1	11,7	15,3	16,9
[6]	10,2	11,8	14,9	16,8
[7]	9,8	12,2	14,2	17,3
[8]	9,9	10,3	15,5	15,5
[9]	10,3	11,1	14,5	16,5
This work	10,4	12,5	15,1	17,8

In addition, by changing the number of evaluation levels of quantization from 256 to 16, the $\frac{E_b}{N_0}$ ratio increases by about 0,8 *dB* and the $\frac{P_s}{P_N}$ ratio – by 1,2 *dB*.

During the numerous experiments, all other parameters were kept constant. While the factors mentioned cause variations in the ratios, it is not possible to identify quantization noise as the primary cause. However, it is evident that quantization noise has a significant share. Figure 4 illustrates the relationship between these parameters $\frac{E_b}{N_0}$ and BER. As can be seen from Table 2, parameters $\frac{E_b}{N_0}$ and $\frac{P_s}{P_N}$ are significantly improved in this work. This proves that the proposed method is an effective method.

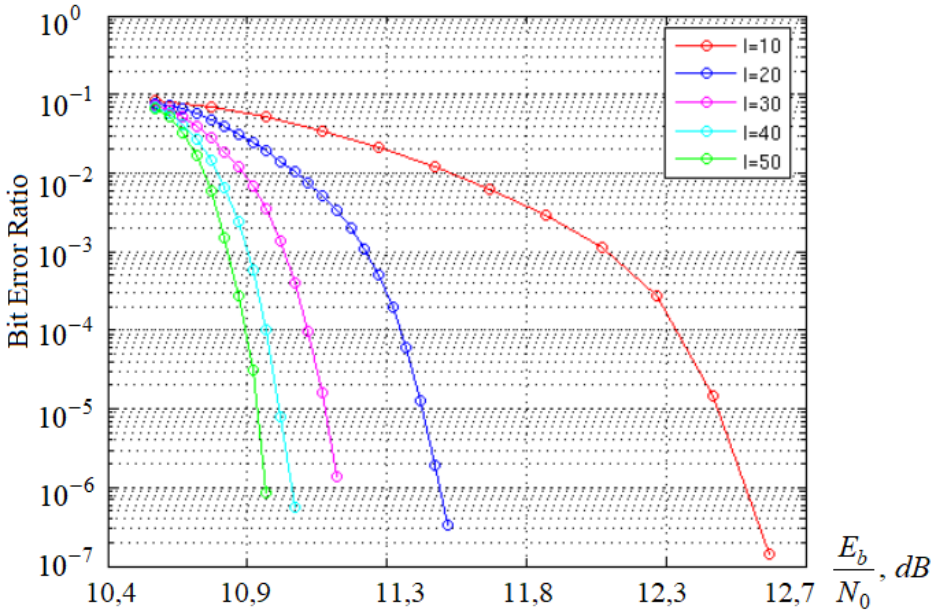

Fig. 4. Dependencies between parameters $\frac{E_b}{N_0}$ and BER.

VI. CONCLUSION

During the quantization of a TV broadcast luminance signal, the level of restriction noise, which arises when the dynamic range of the signal exceeds the allowable quantization level, increases sharply with a rising restriction coefficient. When the distribution of the TV broadcast luminance signal follows an inversely proportional model and a logarithmic quantization scale is applied, the restriction noise power increases 11 times as the restriction factor rises from 1,4 to 1,5. Additionally, when the length of the code word increases from 8 to 10, the ratio of quantization noise power to restriction noise power decreases by approximately 17 times.

ACKNOWLEDGMENT

The authors would like to thank the editor and anonymous reviewers for constructive, valuable suggestions and comments on the work.

REFERENCES

[1] M. Anurag, B. Megha, and S. Arpita, "Video watermarking of live streamed MPEG-4 frames using ELM-Fuzzy-PSO hybrid scheme," *Multimedia Tools and Applications*, vol. 83, pp. 41997-42035, October 2023.

[2] Z. Zhen, J. Wei, Z. Yuan, W. Xiangwen, and Y. Junjie, "Rate-accuracy optimized quantization algorithm based on ROI image coding in power line inspection," *Multimedia Tools and Applications*, vol. 83, pp. 16139-16160, July 2023.

[3] V. F. de Lucena, N. S. Viana, O. B. Maia, J. E. Chaves Filho, and W. S. da Silva, "Designing an extension API for bridging Ginga iDTV applications and home services," *IEEE Trans. Consum. Electron.*, vol. 58, pp. 1077-1085, August 2012.

[4] K. V. da Silva, R. B. de Souza, and de V. F. Jr. Lucena, "A Survey of Digital Television Interactivity Technologies," *Sensors*, vol. 22(17), 6542, July 2022.

[5] M. Dipankar, and T. Panagiotis, "Optimal Controller Synthesis and Dynamic Quantizer Switching for Linear-Quadratic-Gaussian Systems," IEEE Transactions on Automatic Control, vol. 67(1), pp. 382-389, May 2022.

[6] P. P. Sotiriadis, N. Miliou, "Single-Bit Digital Frequency Synthesis via Dithered Nyquist-Rate Sinewave Quantization," *IEEE Transactions on Circuits and Systems*, vol. 61(1), pp. 61-73, February 2021.

[7] D. Pánek, T. Orosz, P. Karban, D. C. D. Gnawa, and H. K. Neghab, "Performance Comparison of Quantized Control Synthesis Methods of Antenna Arrays," *Electronics*, vol. 11, 994, March 2022.

[8] S. Sanghyun, and J. Kim, "Efficient Weights Quantization of Convolutional Neural Networks Using Kernel Density Estimation based Non-uniform Quantizer," *Applied Sciences*, vol. 9(12), 2559, June 2019.

[9] D. Zhang, J. Yang, D. Ye, and G. L. Hua, "Learned Quantization for Highly Accurate and Compact Deep Neural Networks," *European Conference on Computer Vision*, pp. 365-382, June 2018.

[10] R. Babak, A. Azarpeyvand, and A. Khanteymoori, "A Comprehensive Survey on Model Quantization for Deep Neural Networks in Image Classification," *ACM Transactions on Intelligent Systems and Technology*, vol. 14(6), pp. 1-50, November 2023.

[11] H. Khalil, and K. Rose, "Predictive vector quantizer design using deterministic annealing," *IEEE Transactions on Signal Processing*, vol. 51(1), pp. 244-254, November 2023.

[12] O. Shuichi, I. Yuma, and N. Masaaki, Min–Max Design of Error Feedback Quantizers Without Overloading," *IEEE Transactions on Circuits and Systems*, vol. 65(4), pp. 1395-1405, April 2018.

[13] D. N. Thuan, and N. Thinh, "On Binary Quantizer for Maximizing Mutual Information," *IEEE Transactions on Communications*, vol. 68(9), pp. 5435-5445, June 2020.

[14] W. Xinkai, W. Pengjun, Z. Peng, X. Shuzheng, and Y. Huazhong, "A blind audio watermarking algorithm by logarithmic quantization index modulation," *Multimedia Tools and Applications*, vol. 71, pp. 1157-1177, October 2012.

[15] Y. Shengtao, and J. Cheolkon, "Adaptive perceptual quantizer for high dynamic range video compression," *Journal of Visual Communication and Image Representation*, vol. 58, pp. 25-36, January 2019.

[16] L. Yanxiong, Z. Yuhan, L. Xianku, L. Mingle, W. Wucheng, and Y. Jichen, "Acoustic event diarization in TV/movie audios using deep embedding and integer linear programming," *Multimedia Tools and Applications*, vol. 78, pp. 33999-34025, August 2019.

[17] S. J. Mohammed, and Z. S. Hussein, "Design and implementation DVB-S & DVB-S2 systems," *Indonesian Journal of Electrical Engineering and Computer Science*, vol. 20(3), pp. 1444-1452, December 2020.

[18] P. Sathaporn, T. Thanadol, and R. Bundit, "Modulation Error Ratio Gain of Single Frequency Network in DVB-T2," *Electrical, Electronics, Computer and Telecommunications Engineering*, pp. 345-356, January 2019.

[19] W. L. Chih, and T. L. Cheuk, "Vector Quantization With Error Uniformly Distributed

Over an Arbitrary Set," *IEEE Transactions on Information Theory*, vol. 70(7), pp. 5392-5407, April 2024.

[20] M. Hegazy, and C. T. Li, "Randomized quantization with exact error distribution," *Proc. IEEE Inf. Theory Workshop*, pp. 350-355, December 2022.

[21] A.-R. Hussein, and R. Balázs, "Floating-Point Quantization Analysis of Multi-Layer Perceptron Artificial Neural Networks," *Journal of Signal Processing Systems*, vol. 96, pp. 301-312, March 2024.

[22] I.J. Islamov, "Modeling the Attenuation of a Microwave Signal, Taking Into Account the Specific Features of the Terrain for Unmanned Aerial Vehicles," *International Journal of Microwave and Optical Technology*, vol. 18(2), pp. 131-139, March 2023.

[23] I. Islamov, R. Bashirov, and N. Ismayilov, "Modeling of a Telecommunication Optical Waveguide with Anisotropic Medium," *International Journal of Microwave and Optical Technology*, vol. 18(5), pp. 131-139, September 2023.

[24] I. J. Islamov, E. Z. Hunbataliyev, and A. E. Zulfugarli, "Numerical Simulation of Characteristics of Propagation of Symmetric Waves in Microwave Circular Shielded Waveguide with a Radially Inhomogeneous Dielectric Filling," *International Journal of Microwave and Wireless Technologies*, vol. 9, pp. 761-767, July 2022.

[25] F. Toshiyuki, K. Yuhji, S. Michiyuki, and Y. Yasuhiro, "Real-Life In-Home Viewing Conditions for Flat Panel Displays and Statistical Characteristics of Broadcast Video Signal," *Japanese Journal of Applied Physics*, vol. 46, 1358, March 2007.

[26] Z. Jin, L. Zhiping, Z. Cheng, Y. Xianxun, Y. Baohua, S. Xiaozhou, and M. Jungang, "Analog–digital conversion signal-to-noise ratio analysis for synthetic aperture interferometric radiometer," *Journal of Applied Remote Sensing*, vol. 8(1), 083635, May 2014.

[27] Yu. E. Korchagin, K. D. Titov, and O. N. Zavalishina, "Detection of Phase Modulation Disorder of Narrowband Radio Signals Against a Background of White Gaussian Noise," *Radio Electronics, Electrical and Power Engineering*, pp. 456-465, May 2024.

[28] A. S. Glinchenko, A. M. Aleshechkin, and V. A. Komarov, "Increasing the Reliability of Spectral Measurements of Signal Parameters at Low Signal-to-Noise Ratios," *Measurement Techniques*, vol. 58, pp. 1054-1061, December 2015.

[29] M. Suba, and D. Susan, "Performance analysis of cyclostationary spectrum sensing with dynamic thresholding using artificial neural network under varying signal to noise ratio and noise variance conditions," *Journal of Intelligent & Fuzzy Systems*, vol. 45(2), pp. 3247-3257, August 2023.

[30] I. Peshkov, "Simulation Study of Digital Spatial Processing in Conditions of Tropospheric Propagation of Radio Waves for Telecommunication Applications," *Progress In Electromagnetics Research C*, vol. 143, pp. 109-119, May 2024.

[31] I. Islamov, "Optimization of Broadband Microstrip Antenna Device for 5G Wireless Communication Systems," *Transport and Telecommunication*, vol. 24(4), pp. 409-422, November 2023.

[32] I. Islamov, and A. Safarli, Design, "Modelling and Research of an Antenna System for Transmitting and Receiving Information in Satellite Systems," *Transport and Telecommunication*, vol. 24(3), pp. 297-308, June 2023.

[33] Y. Sanghun, K. Bong-seok, and K. Sangdong, "A Robust Super-Resolution Algorithm in a Low SNR Environment for Vital Sign Radar," *Radioengineering*, vol. 33(1), pp. 155-162, April 2024.

[34] K. P. Malygin, and A. V. Nosov, "Effect of the Distance Between the Non-Core Turns of a Meander Microstrip Line on the Attenuation of the Interfering Ultrashort Pulse and Signal Integrity," *IEEE Electromagnetic Compatibility Magazine*, vol. 12(3), pp. 45-54, December 2023.

[35] G. Mohammed, A. Aishy, and G. Ali, "A Fast Directional Sigma Filter for Noise Reduction in Digital TV Signals," *IEEE Transactions on Consumer Electronics*, vol. 53(4), pp. 1500-1507, November 2007.

[36] I.R. Mammadov, Z.A. Ismailov, "Noise power limitations when transmitting TV broadcast signals over digital communication systems," *Modern television and radio electronics*, 2013, pp. 45-48, November 2013.